# Layer-by-Layer Self-Assembly of Polyelectrolyte-Semiconductor Nanoparticle Composite Films

**ARTICLE** *in* THE JOURNAL OF PHYSICAL CHEMISTRY · AUGUST 1995

Impact Factor: 2.78 · DOI: 10.1021/j100035a005



**3 AUTHORS**, INCLUDING:

Nicholas Kotov
University of Michigan
**445** PUBLICATIONS **27,111** CITATIONS

SEE PROFILE

I. Dekany
University of Szeged
**352** PUBLICATIONS **8,860** CITATIONS

SEE PROFILE

# Layer-by-Layer Self-Assembly of Polyelectrolyte-Semiconductor Nanoparticle Composite Films

Nicholas A. Kotov, Imre Dekany, and Janos H. Fendler

*J. Phys. Chem.*, **1995**, 99 (35), 13065-13069• DOI: 10.1021/j100035a005 • Publication Date (Web): 01 May 2002

# Layer-by-Layer Self-Assembly of Polyelectrolyte−Semiconductor Nanoparticle Composite Films

**Nicholas A. Kotov,[†] Imre Dékány,[‡] and Janos H. Fendler*,[†]**

*Department of Chemistry, Syracuse University, Syracuse, New York 13244-4100, and Department of Colloid Chemistry, Attila József University, Aradi Vt., t. 1., H-6720, Szeged, Hungary*

*Received: June 13, 1995*[⊗]

Spectroscopic (absorption and emission), microscopic (transmission electron and atomic force), X-ray diffraction and photocurrent measurements have provided evidence for the formation of stable ultrathin films with regular periodicities, by the layer-by-layer self-assembly of polycations and cadmium sulfide, lead sulfide and titanium dioxide nanoparticles.

## Introduction

Formation of Langmuir films from nanosized clay platelets,[1] semiconductor,[2,3] metallic,[4−6] magnetic,[7] and ferroelectric[8] particles on aqueous solution surfaces and their layer-by-layer transfer onto solid substrates by the Langmuir−Blodgett technique have provided a viable route for the construction of advanced materials by colloid chemical methodologies.[9,10] Self-assembly of functionalized surfactants on gold or silver substrates[11] and the sequential adsorption of oppositely charged polyelectrolytes,[12−16] polyelectrolytes and clay platelets,[17] polyelectrolytes and exfoliated zirconium phosphate,[18] and polyelectrolytes and metal colloids[19] on a variety of substrates have permitted an alternative approach. The relative ease of preparation and versatility have contributed to the rapid burgeoning of these latter procedures.

Evidence is presented in this letter for the self-assembly of ordered nanostructured films, composed of alternative layers of cationic poly(diallylmethylammonium chloride) and negatively charged semiconductor particles onto a variety of substrates, including Teflon. Thiol and sodium hexametaphosphate-stabilized lead sulfide (PbS), titanium dioxide ($TiO_2$), and highly fluorescent cadmium sulfide (CdS) particles were used as semiconductors. Photocurrent measurements of composite nanostructured films indicated a marked dependence on the sequence in which the CdS and $TiO_2$ particles were layered.

## Experimental Section

CdS and PbS nanoparticles were prepared in aqueous dispersions by using a mixture of thiolactic acid (TLA) and ethylmercaptane (EM) as a stabilizer. The optimum mixture was found by systematically varying the mole fraction of TLA to EM. Self-assembly of nanoparticles was found to be the most efficient in a TLA:EM = 1:3 ratio. Typically, appropriate amounts (0.1−1.5 mL) of TLA and EM were dissolved in 100 mL of water. The pH of the solution was adjusted with 2.0 M NaOH to 9.5−10.2. The metal salt ($Cd(ClO_4)_2 \cdot 6H_2O$ or $Pb(NO_3)_2$) was dissolved in 100-mL deionized water and added slowly to the aqueous solution of the stabilizers. The combined solution of precursors was purged with Ar for at least 20 min prior to the addition of $Na_2S$ (0.053−0.24 g). A substantial excess (1.5−10 times) of metal ions over a stoichiometric amount of $S^{2-}$ ions was maintained to ensure efficient binding of the stabilizer to the nanoparticles. Normally, a clear slightly yellow (CdS) or black (PbS) dispersion was obtained in the synthesis. The absorption spectra of CdS dispersions revealed the presence of a sharp absorption edge. These results indicated a rather narrow size distribution of the nanoparticles (ca. 20% dispersion around the mean diameter).[20] Refluxing at 100 °C was found to stimulate the growth of particles while maintaining a narrow size distribution. This process was used to vary the diameter of the nanoparticles in the self-assembled films. The sizes of the PbS particles were also found to increase upon heating, reaching the limit in ca. 2 h. However, the size distribution of these particles was always broad and was found too hard to manipulate.

$TiO_2$ nanoparticles were synthesized by the slow injection of 1.5 mL of titanium isopropoxide (0.005 mol) into 300 mL of water in the presence of 0.1 g of poly(acrylic acid) (PAA; pH = 10.5). The immediate formation of a slightly opaque, colloidal dispersion was observed. After aging for 24 h, a portion of the stock solution was subjected to centrifugation and then used for self-assembly. The average particle size in the dispersion was estimated to be 25 Å by absorption spectroscopic measurements.

Na-montmorillonite was prepared according to standard procedures.[1] The stock clay dispersion was produced by sonication (Braunsonic 2200 sonication bath) of a desired amount of dry Na-montmorillonite (0.2−1.0 g) in 100 mL of deionized water (from a Millipore Milli-Q system) for 40 min. Then, the mixture was subjected to centrifugation at ca. 1500 rotations/min for 2 h. The solid precipitate was collected, and the transparent supernatant was used for further experiments.

The substrates (S; quartz, glass, gold, platinum, and Teflon) that were used for self-assembly were cleaned by immersion in Nocromix solution in concentrated sulfuric acid for 0.5−3 h. The construction of a polycation−semiconductor particle sandwich unit, illustrated for CdS, involved the following steps: (i) immersion of S into a 1.0%, w/v, aqueous cationic poly(diallylmethylammonium chloride) (P) solution, kept at pH = 8.5 (no buffer), for 15 min; (ii) rinsing with a stream of deionized distilled water, kept at pH = 8.5 or 10.0 for PbS; (iii) immersion into an aqueous semiconductor nanoparticle dispersion, kept at pH = 9−10, for 24 h; (iv) washing with a stream of deionized water, kept at pH = 8.5 or 10.0 for PbS. Each washing was followed with drying by a stream of $N_2$ for 30 s. Thus, performing steps i−iv led to the self-assembly of a one layer of polycation−one layer of CdS nanoparticle sandwich unit on the substrate, for which we adopted the S−(P/CdS) short-hand notation. Subsequent polycation-CdS nano-

[†] Syracuse University.
[‡] Attila József University.
[⊗] Abstract published in *Advance ACS Abstracts,* August 15, 1995.

0022-3654/95/2099-13065$09.00/0 

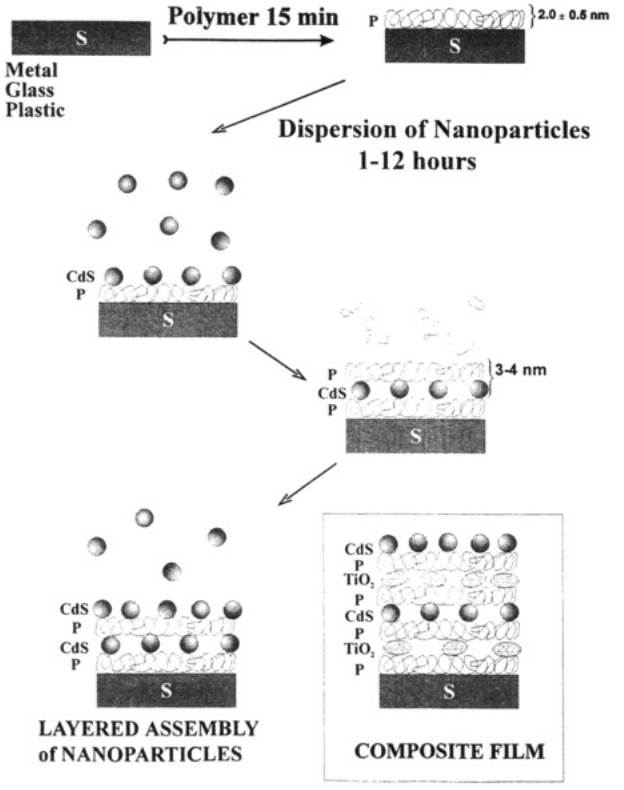


**Figure 1.** Schematics of the self-assembly of ultrathin films composed of alternating layers of polycations (P)−semiconductor nanoparticles (CdS) and composite polycation (P)−semiconductor nanoparticles (CdS or $TiO_2$; in the box) on metal, glass or plastic substrates (S).

particle sandwich units were self-assembled by repeating steps i−v $n$ times to produce films comprised of $n$ number of sandwich units, $S-(P/CdS)_n$. The schematics of the self-assembly of an $S-(P/CdS)_n$ film are illustrated in Figure 1. Similar methodologies (steps i−iv) were employed for the self-assembly of $S-(P/PbS)_n$ and $S-(P/TiO_2)_n$ films.

Water was purified by a Millipore Milli-Q system containing a 0.22-$\mu$m Millistack filter at the outlet.

X-ray diffraction measurements were performed by a Phillips PW 1830 diffractometer (Cu K$\alpha$, $\lambda = 1.54$ Å). The quartz, glass, ITO-coated glass, and Teflon plates, used as substrates, were found not to have peaks in the region of interest. Fluorescence spectra were taken on a Tracor-Northern 6500 rapid scan spectrofluorometer system.

Photocurrents were measured by illuminating the self-assembled, film-carrying Pt electrode by a defocused light (100 W Hg lamp). Defocused light was used to avoid heating the sample surface, which could have caused a substantial nonfaradaic current. The photocurrent was registered at potentiostatic conditions, $\Delta V = 0.6$ V (Ag/AgCl standard). A magnitude of the photocurrent reached a constant level ($I_{photo}$), which was used to characterize $TiO_2$, composite $TiO_2$/CdS, and $TiO_2$/CdS/M films. The initial maximum of the photocurrent was found to depend on the frequency of dark/light periods, whereas $I_{photo}$ was affected only by the structure of the self-assembled semiconductor film on the electrode (i.e., number of layers, sequence of particles, etc.).

Surface plasmon spectroscopic measurements were carried out by using a home-constructed system. Gold or silver (vacuum evaporated to 40−50 nm thickness) coated glass slides were used as the reflection element. The uncoated side of the slide was brought into optical contact with the base of a 90° glass prism ($n = 1.52$) by an index matching oil ($n = 1.518 \pm 0.0005$). A p-polarized, 632.8-nm beam was directed to the base of the prism by a HeNe Laser (Hughes, 3235H-PC, ca. 20 mW). The prism was mounted on a stepping motor-driven rotator (Oriel) that was capable of synchronously varying the angle of incidence ($\theta$) and the direction of a large area silicon detector (Newport, 818-SL) with an angle resolution of 0.01°. The angular sample interval was 0.05° within 2° of the resonance minimum and 0.2° elsewhere. Angular reflection scans required about 20 min. Each angular scan was fitted to a theoretical reflection curve, calculated by choosing appropriate one-, two-, or three-layer models and refractive indexes.

Transmission electron micrographs (TEM) were taken either on a JEOL 2000-FX electron microscope operating at 200 keV or on a JEOL 2000-EX electron microscope operating at 120 keV. Formvar-covered, carbon-coated, 200-mesh copper grids were allowed to float on the surface of a 2% polyelectrolyte solution for 12 h. Care was taken to avoid contact of the uncoated grid face with the aqueous solution. After copious rinsing with water, the grids were put in the same manner on a dispersion of montmorillonite which was analogous to the one that was used for the priming of other substrates. This step was followed by rinsing and self-assembly of polyelectrolytes in an identical procedure. After that, the grids were ready for the self-assembly of semiconductor particles, which proceeded by floating on the surface of an aqueous dispersion of nanoparticles for 24 h. Once again, care was taken to avoid deposition of self-assembled films on both sides of the grid.

AFM images were taken by a Topometrix Explorer 2000 scanning probe microscope with standard silicon nitride tips (force constant of 0.12 N/m) in the contact, as well as in the noncontact modes. Freshly cleaved mica was used as the substrate for AFM measurements.

## Results and Discussion

Demonstration of a versatile method of layer-by-layer self-assembly of polycations and semiconductor nanoparticles into stable ultrathin films is the most significant accomplishment of the present work (Figure 1). Cationic poly(diallyldimethylammonium chloride) (P) was found to adhere strongly to a variety of surfaces. Indeed, immersion of a quartz slide, a platinum or gold electrode, an ITO-coated glass, a freshly cleaved sheet of mica, and even a Teflon film into a 1.0% aqueous solution of P resulted in the adhesion of the polyelectrolyte onto these substrates. The thickness of P, self-assembled on a gold electrode, was determined to be $2.0 \pm 0.5$ nm by surface plasmon spectroscopy. Furthermore, soaking in aqueous solution for hours did not remove P, as evidenced by the unaltered surface plasmon spectrum. AFM images of the polyelectrolyte film revealed featureless, wavelike structures with height variations of about 2 nm. Apparently, strong van der Waals forces maintain P on a variety of substrate surfaces, even in the absence of covalent bonding. It should be pointed out that polyelectrolytes were not directly self-assembled onto substrates previously. Typically, the substrates were silanized or coated by a functionalized monolayer, transferred by the Langmuir−Blodgett technique, prior to its immersion into the polyelectrolyte solution.[12−16]

Self-assembly of the negatively charged, surfactant-stabilized CdS, PbS, and $TiO_2$ nanoparticles onto the positive surface of P was greatly facilitated by strong electrostatic interactions. Assuming the polycation to be completely stretched on the surface of S, the mean area occupied by a positive charge on P can be estimated to be 10 Å$^2$. The corresponding mean distance between negative charges on the semiconductor nanoparticle surface is somewhat harder to estimate. We can assume a fairly dense packing of stabilizer molecules in a fashion similar to

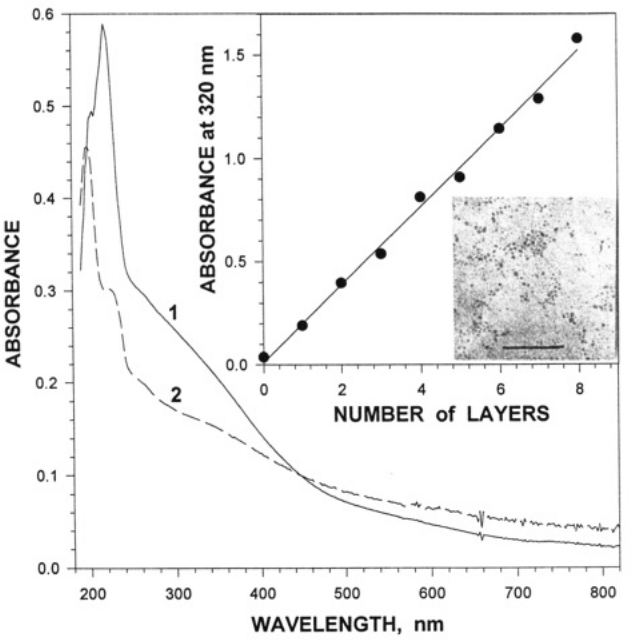


**Figure 2.** Absorption spectrum of PbS nanoparticle dispersions in aqueous solutions (1) and that of one monoparticle layer of PbS self-assembled onto one layer of polycation-coated quartz substrate (2). The absorbances at 224 nm vs the number of sandwich units ($n$) in S−(P/CdS)$_n$ are plotted in the insert. Transmission electron micrographs of one layer of PbS self-assembled onto one layer of polycation-coated substrate are also shown in the insert. The scale bar is 100 nm.

self-assembled thiol monolayers on gold. Recent NMR and XPS data substantiate this assumption.[21] It is important to mention that only one of the stabilizers used (TLA) carries a charge. Consequently, the area per negative charge will depend on the TLA:ET ratios. Nevertheless, the upper limit of the area occupied by a negative charge can be estimated to be about 50 Å$^2$. Taking only half of the particle surface area facing the plane of adsorption, the minimum number of the interaction sites between the positive P and negative semiconductor particles is estimated to be about 20. This number can be much greater, of course. However, it is essential to point out that a highly charged surface does not necessarily ensure efficient self-assembly. The higher the charge of a nanoparticle, the higher its affinity toward water. Consequently, the Gibbs free energy of a nanoparticle does not change substantially upon adsorption on a polyelectrolyte film, and hence it can also be easily desorbed by subsequent washing. Finding a proper balance between charge (to provide attraction to the polyelectrolyte layer) and hydrophobicity (to prevent lability of adsorbed species) is, therefore, of paramount importance for the optimization of self-assembly. This condition, for the present system, was found for a 1:3 = TLA:ET ratio by the maximization of the optical density of one self-assembled layer.

The absorption spectra of the CdS (not shown) and PbS (Figure 2) nanoparticle dispersions in aqueous solutions are retained in the self-assembled films. Furthermore, the absorption edges (ca. 430 nm for CdS and ca. 500 nm for PbS) correspond to mean particle diameters of 35 and 100 Å. That these particles are indeed in the nanometer region and are, thus, size quantized can also be seen in their transmission electron micrographs (insert in Figure 2).

AFM images of self-assembled $TiO_2$ particles (Polysciences, Inc.; size = 100 nm) revealed the formation of a well-packed monoparticle layer (Figure 3). The tight packing of the $TiO_2$ particles precluded the penetration of the AFM tip to the mica surface. The image of the film was quite similar in all acquisition modes used (topography, internal sensor, beam deflection, lateral force, and $z$ force). Interestingly, lateral force microscopy provided the most detailed images. In the topog-

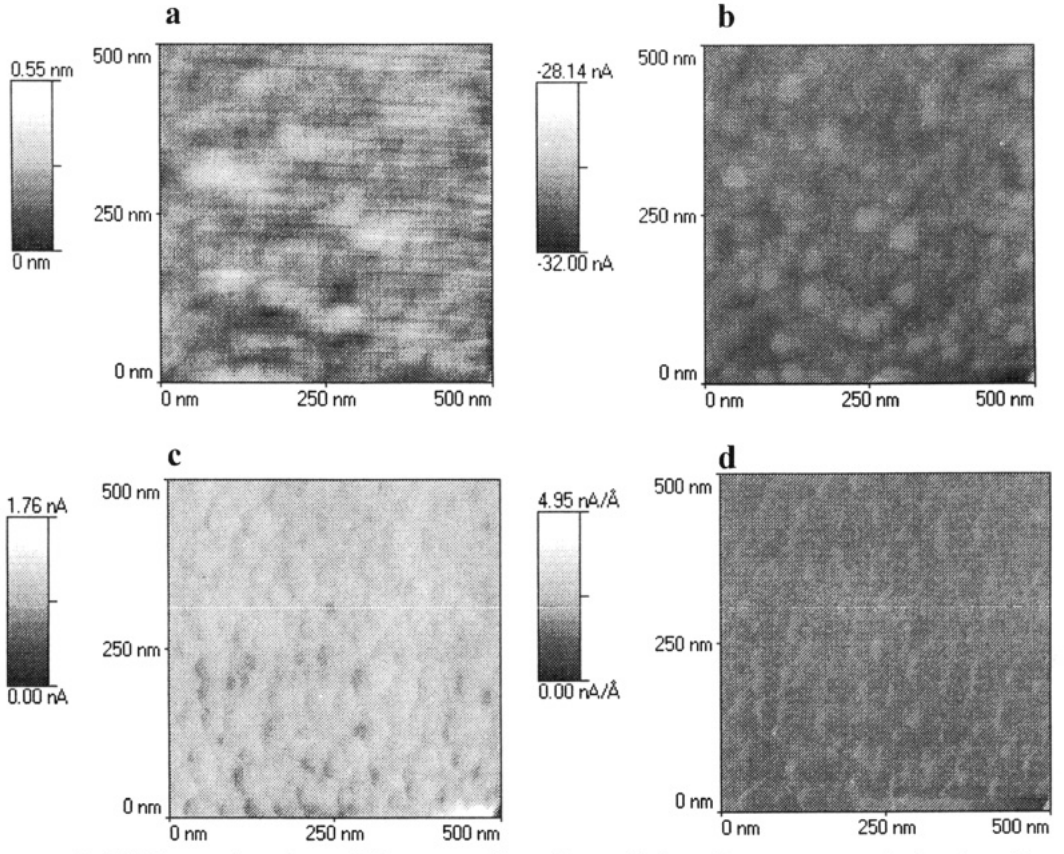


**Figure 3.** Contact-mode AFM images of one layer of $TiO_2$ nanoparticles self-assembled on mica. a = topography, b = internal sensor, c = lateral forces and d = hardness. Set point = −10 nA, scan rate = 200 nm/s, resolution = 200 lines.

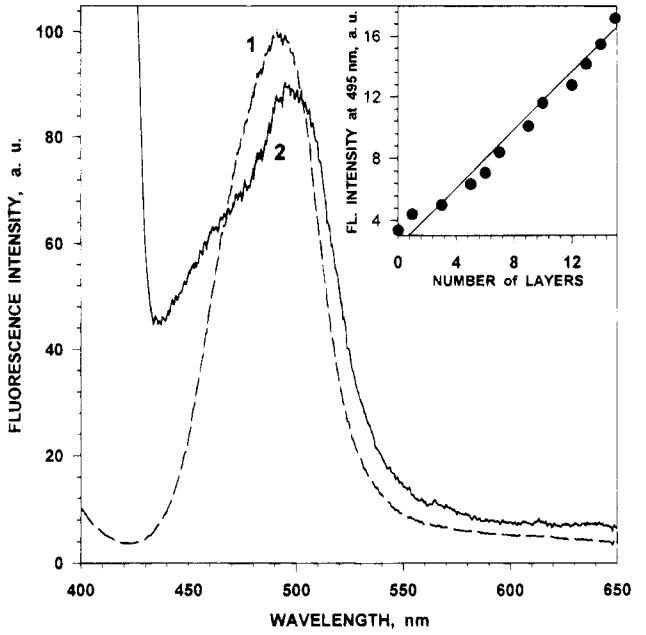


**Figure 4.** Emission spectrum of CdS nanoparticle dispersions in aqueous solutions (1) and that of S−(P/CdS)$_{20}$ self-assembled onto a Teflon film (2). $\lambda_{ex}$ = 360 nm, frontface illumination. The fluorescence intensities at 495 nm vs the number of sandwich units ($n$) in S−(P/CdS)$_n$ are plotted in the insert.

raphy mode, the images that were obtained tended to have enlarged features. These observations indicate the presence of rather strong van der Waals forces between the AFM tip and the $TiO_2$ particles.

The successful self-assembly of a large number of repeating sandwich units of S−(P/CdS)$_n$, S−(P/PbS)$_n$, and S−(P/TiO$_2$)$_n$ was monitored by absorption and emission spectroscopic measurements. For example, the observed good linearities in the plots of absorbances vs $n$ in S−(P/PbS)$_n$ indicate the uniformity of the sandwich units that were self-assembled (see insert in Figure 2). Activated CdS nanoparticle dispersions showed a strong fluorescence with an emission maximum at 490 nm, which was attributed to the $1s_e-1s_h$ exitonic transition.[22] Very similar emission spectra were obtained for the self-assembled S−(P/CdS)$_n$ films (Figure 4). Furthermore, the relative intensity of the emission was found to increase linearly with increasing P/CdS units, self-assembled on the substrate, up to $n$ = 18 (see insert in Figure 4). The good linearity of the fluorescence intensity vs $n$ plot indicates the uniformity of the self-assembled film. This was also confirmed by X-ray diffraction of a S−(P/CdS)$_{20}$ sample. The observed $2\theta$ = 1.70 peak (not shown) corresponded to a 6.5 ± 0.8 nm repeating unit in the (P/CdS)$_{20}$ film. Since the CdS particle diameters were determined to be 4.0 ± 0.5 nm, the difference (6.5 ± 0.8 nm − 4.0 ± 0.5 nm = 2.5 ± 1.3 nm) agrees well with that determined for the thickness of a polyelectrolyte layer by surface plasmon spectroscopy (2.0 ± 0.5 nm, vide supra).

Self-assembly allows the construction of composite films comprising different nanoparticles that can be layered in any desired order. Under irradiation, the S−(P/TiO$_2$)$_n$ and any combination of the mixed P/TiO$_2$ and P/CdS self-assembled films behaved like typical n-type semiconductors (Figure 5), whose properties were determined by the development of a depletion layer at the semiconductor−electrolyte interface.[23] It should be noted that the nanoparticles investigated here are too small to allow full development of the depletion layer, whose thickness is supposed to be about 100 nm for $TiO_2$. It is

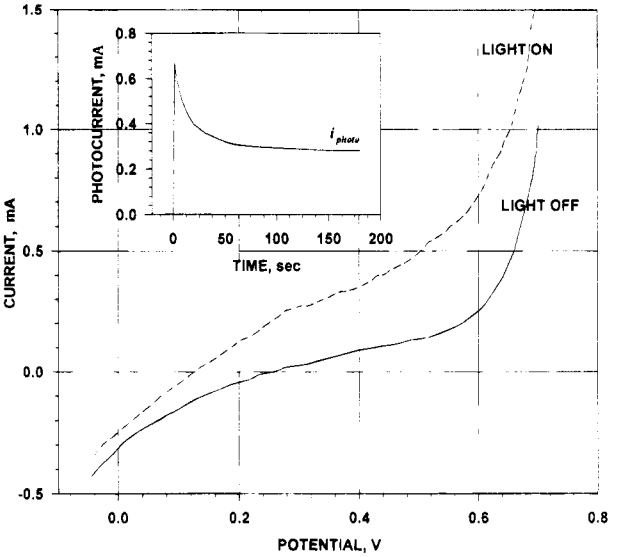


**Figure 5.** Current vs potential plots, in the dark and under illumination, in a photoelectrochemical cell using a working electrode, prepared by self-assembling ten layers of $TiO_2$, S−(P/TiO$_2$)$_{10}$. Scan rate = 0.5 mV/s. Illumination onto the platinum electrode was provided by a defocused 100 W Hg lamp. A typical photocurrent is illustrated in the insert. The current in the first couple of seconds originates from the oxidation of water and a small amount of adsorbed impurities. Hence, the peak photocurrent observed was found to depend on the sample history (extent of previous irradiation). However, the plateau value of the photocurrent ($i_{photo}$) was independent of the sample history and was reproducible (within 10%) for a given sample in the same electrolyte solution under the same extent of irradiation.

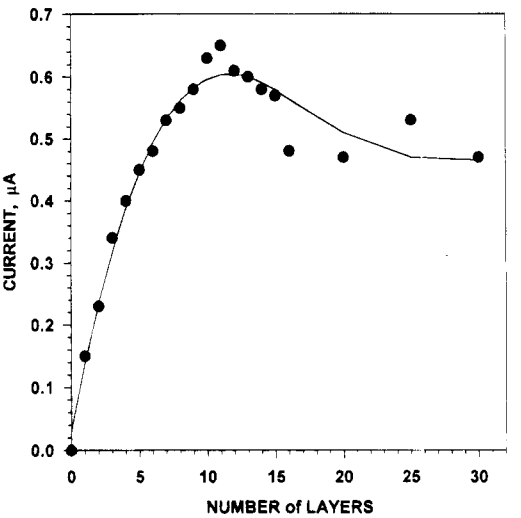


**Figure 6.** Photocurrent vs the number of sandwich units ($n$) in S−(P/TiO$_2$)$_n$.

conceivable that, in our semiconductor films, the whole assembly, consisting of multiple layers, behaves as one electronic unit. The photoinduced current is caused by photogenerated holes (minority carriers). At positive electrode potentials, they accumulate and oxidize water molecules. The plateau value of the photocurrent ($i_{photo}$) for a P/TiO$_2$ unit, deposited up to a maximum at S−(P/TiO$_2$)$_{15}$, decreased somewhat beyond it (Figure 6).

The effects of organization of P/CdS and P/TiO$_2$ on the measured photocurrents ($i_{photo}$) are summarized in Table 1. Introduction of one to three layers of insulating polyelectrolyte−montmorillonite (P/M) between layers of P/TiO$_2$ had the expected consequence of photocurrent decrease. Aluminosilicate platelets block the movement of photogenerated charge

**TABLE 1: Photocurrents in Differently Organized Composite Semiconductor Nanostructures**

| structure of the working electrode[a] | $i_{photo}$,[b] μA |
|---|---|
| $S-(TiO_2/P)_{10}$ | 0.63 |
| $S-(M/P)_3(TiO_2/P)_{10}$ | 0.10 |
| $S-(TiO_2/P)_2(M/P)_3(TiO_2/P)_8$ | 0.23 |
| $S-(TiO_2/P)_5(M/P)_3(TiO_2/P)_5$ | 0.40 |
| $S-(TiO_2/P)_8(M/P)_3(TiO_2/P)_2$ | 0.47 |
| $S-(TiO_2/P)_{10}(M/P)_3$ | 0.63 |
| $S-(TiO_2/P)(CdS/P)(TiO_2/P)_2(CdS/P)-(TiO_2/P)_2(CdS/P)(TiO_2/P)_2(CdS/P)(TiO_2/P)_2(CdS/P)(TiO_2/P)$ | 0.43 |
| $S-(TiO_2/P)_{10}(CdS/P)_5$ | 0.23 |

[a] S = substrate; M = montmorillonite; $TiO_2$ = titanium dioxide; CdS = cadmium sulfide. The subscript number following the parentheses indicates the number of repeating units which were self-assembled. [b] $i_{photo}$ = plateau value photocurrent.

carriers within the film and, thus, diminish the photocurrent. A correlation between the position of P/M and the photocurrent was observed. The further the P/M layer was placed from the electrode, the greater the photocurrent became. The transparent P/M film does not affect light absorption in the film, but it divides the composite film into active and nonactive parts. The part adjacent to the electrode is responsible for the generation of the photocurrent. The closer the active part of the film to the electrode, the greater the photocurrent.

The spontaneous, layer-by-layer self-assembly of polyelectrolyte–semiconductor particle nanostructured films, reported here, exemplifies well our proposed membrane–mimetic approach to advanced materials.[9] While the dimensions, organization, and deceptive simplicity of spontaneous self-assembly are analogous to the corresponding properties of the biological membrane, the present system offers versatility and a relative ease of systematic physical and chemical manipulation. Judicious selection of components and their layer-by-layer self-assembly will result in nanostructured films with the desired mechanical, optical, electrooptical, electrical, magnetic, and electromagnetic properties.

**Acknowledgment.** Support of this work by grants from the National Science Foundation (U.S.A.) and the U.S.–Hungarian Joint Fund (Hungary) is gratefully acknowledged. We thank Dr. Y. Yuan for help with TEM.

## References and Notes

(1) Kotov, N. A.; Meldrum, F. C.; Fendler, J. H.; Tombácz, E.; Dékány, I. *Langmuir* **1994**, *10*, 3797.
(2) Kotov, N. A.; Meldrum, F. C.; Wu, C.; Fendler, J. H. *J. Phys. Chem.* **1994**, *98*, 2735.
(3) Kotov, N. A.; Meldrum, F. C.; Fendler, J. H. *J. Phys. Chem.* **1994**, *98*, 8827.
(4) Kotov, N. A.; Meldrum, F. C.; Fendler, J. H. *Langmuir* **1994**, *10*, 2035.
(5) Meldrum, F. C.; Kotov, N. A.; Fendler, J. H. *J. Chem. Soc., Faraday Trans.* **1994**, *90*, 673.
(6) Meldrum, F. C.; Kotov, N. A.; Fendler, J. H. *Chem. Mater.*, in press.
(7) Meldrum, F. C.; Kotov, N. A.; Fendler, J. H. *J. Phys. Chem.* **1994**, *98*, 4506.
(8) Kotov, N. A.; Zavala, G.; Fendler, J. H. *J. Phys. Chem.*, in press.
(9) Fendler, J. H. *Membrane-Mimetic Approach to Advanced Materials*; Springer-Verlag: Berlin, 1994; Advances in Polymer Science Series, Vol. 113.
(10) Fendler, J. H.; Meldrum, F. C. *Adv. Mater.*, in press.
(11) Ulman, A. *An Introduction to Ultrathin Organic Films from Langmuir Blodgett to Self-Assembly*; Academic Press Inc.: Boston, 1991.
(12) Cheung, J. H.; Punkka, E.; Rikukawa, M.; Rosner, R. B.; Royappa, A. T.; Rubner, J. F. *Thin Solid Films* **1992**, *210/211*, 246.
(13) (a) Schmitt, J.; Grünewald, T.; Kjaer, K.; Pershan, P.; Decher, G.; Lösche, M. *Macromolecules* **1993**, *26*, 7058. (b) Lvov, Y.; Essler, F.; Decher, G. *J. Phys. Chem.* **1993**, *97*, 13773. (c) Decher, G.; Hong, J. D. *Ber. Bunsen-Ges. Phys. Chem.* **1991**, *95*, 1430.
(14) Iler, R. K. *J. Colloid Interface Sci.* **1966**, *21*, 569.
(15) Ingersoll, D.; Kulesza, P. J.; Faulkner, L. R. *J. Electrochem. Soc.* **1994**, *141*, 140.
(16) Mao, G.; Tsao, Y.; Tirell, M.; Davis, H. T.; Hessel, V.; Ringsdorf, H. *Langmuir* **1993**, *9*, 3461.
(17) Kleinfield, E. R.; Ferguson, G. S. *Science* **1994**, *265*, 370.
(18) Keller, S. W.; Kim, H.-N.; Mallouk, T. E. *J. Am. Chem. Soc.* **1994**, *116*, 8817.
(19) Freeman, R. G.; Grabar, K. C.; Allison, K. J.; Bright, R. M.; Davis, J. A.; Guthrie, A. P.; Hommer, M. B.; Jackson, M. A.; Smith, P. C.; Walter, D. G.; Natan, M. J. *Science* **1995**, *267*, 1629.
(20) (a) Weller, H. *Adv. Mater.* **1993**, *5*, 88. (b) Hodes, G. *Isr. J. Chem.* **1993**, *33*, 95.
(21) (a) Sachleben, J. R.; Wooten, E. W.; Emsley, L.; Pines, A.; Colvin, V. L.; Alivisatos, P. *Chem. Phys. Lett.* **1992**, *198*, 43. (b) Becerra, L.; Murray, C. B.; Griffin, R. G.; Bawendi, M. G. *J. Chem. Phys.* **1994**, *100*, 3297. (c) Bowen Katari, J. E.; Colvin, V. L.; Alivisatos, A. P. *J. Phys. Chem.* **1994**, *98*, 4109.
(22) Tian, Y.; Newton, T.; Kotov, N. A.; Guldi, D. K.; Fendler, J. H., unpublished results, 1995.
(23) McHardy, J.; Ludwig, F. *Electrochemistry of Semiconductors and Electronics Processes and Devices*; Noyes Publications: Park Ridge, NJ, 1992.

JP951653I